

Micro-Raman imaging analysis of monomer/mineral distribution in intertubular region of adhesive/dentin interfaces

Yong Wang

University of Missouri-Kansas City
School of Dentistry
650 E. 25th St.
Kansas City, Missouri 64108
E-mail: Wangyo@umkc.edu

Paulette Spencer

University of Missouri-Kansas City
School of Dentistry
and
Department of Pediatric Dentistry
650 E. 25th St.
Kansas City, Missouri 64108

Xiaomei Yao

University of Missouri-Kansas City
School of Dentistry
650 E. 25th St.
Kansas City, Missouri 64108

Abstract. It is generally proposed that bonding of resins to dentin results from infiltration of the adhesive monomers into the superficially demineralized dentin. However, it is still not clear how well the mineral phase of dentin is removed and how far each monomer penetrates into the thin zone of “wet” demineralized dentin. The quality and molecular structure of adhesive/dentin interfaces formed under “wet” bonding conditions are studied using 2-D Raman microspectroscopic mapping/imaging techniques. Micro-Raman imaging analysis of the adhesive/dentin interface provides a reliable and powerful means of identifying the degree and depth of dentin demineralization, adhesive monomer distribution, and flaws or defects in the pattern of adhesive penetration. The image of mineral reveals a partially demineralized layer on the top of dentin substrate. Adhesive monomers readily penetrate into dentin tubules and spread into intertubular region through open tubules. The extent of adhesive monomer penetration is higher in the intertubular regions close to tubules as compared to the middle regions between the tubules. The diffusion of resin monomers differs substantially. In a comparison with a hydrophilic monomer, the hydrophobic monomer resists diffusion into the demineralized intertubular dentin area. © 2006 Society of Photo-Optical Instrumentation Engineers. [DOI: 10.1117/1.2187992]

Keywords: dentin; adhesive; spectroscopy; Raman; imaging.

Paper 05317R received Oct. 24, 2005; revised manuscript received Dec. 28, 2005; accepted for publication Dec. 29, 2005; published online Mar. 27, 2006.

1 Introduction

Current dentinal adhesive systems that acid etch the dentin characteristically bond via resin infiltration, polymerization, and entanglement of exposed collagen in the demineralized dentin zone.¹ This distinct zone has been labeled the resin-collagen hybrid layer.^{2–5} With removal of the mineral phase by acid etching, the exposed collagen fibers are suspended in water and will collapse after drying.^{6,7} A collapsed collagen network reduces the porosity and inhibits resin penetration through the demineralized layer,⁶ thus, a wet bonding technique has been frequently used to maintain the porosity of the demineralized dentin.^{8,9} It is suggested that the higher bond strengths with this technique are related to the greater resin infiltration into a more porous collagen network.^{6,9,10} The initial increase in bond strength of adhesive applied using wet bonding techniques is not, however, maintained over time.^{11,12} For example, an *in vivo* study¹² showed that mean tensile bond strength values dropped from 28.3 MPa at 24 h to 9.1 MPa at 2 to 3 yr. The initially high bond strength values recorded with wet bonding techniques do not necessarily indicate an adhesive/dentin bond that is stable in aqueous envi-

ronments. The factors and mechanisms involved in the premature failure of this adhesive/dentin bond remain unclear.

The durability of the adhesive/dentin bond is directly related to the quality of the interface that connects the bulk composite/adhesive to the subjacent, intact dentin. Understanding the factors that determine quality of the interface depends on comprehensive characterization of the dynamic reactions that occur in dentin substrates during acid etching and bonding. Determining the composition/structure of the hybrid layer has been a formidable problem, and currently the majority of our techniques have provided only an indirect morphological assessment. High-resolution analytical techniques that enable direct, nondestructive, *in situ* detection of molecular structures and provide us with the capability of measuring this information at a spatial resolution approximately equivalent to this thin zone (~1 to 10 μm) are necessary. Micro-Raman spectroscopy has proven^{4,13–15} to be well suited to the characterization of the chemical structure and character of adhesive resins, collagen, and minerals at a resolution up to 1 μm .

The adhesive/dentin interface investigation resulted in increased attention to dentin structure, the detailed information of which is essential for interpreting data from studies on dentinal adhesive resins. The strength of the bonds between

Address all correspondence to Yong Wang, University of Missouri at Kansas City, Department of Oral Biology, 650 E. 25th St., Kansas City, Missouri 64108. Tel: 816-235-2043; Fax: 816-235-5524; E-mail: Wangyo@umkc.edu

adhesive and dentin is influenced by the number, size, and orientation of dentinal tubules as well as the relative amount of intratubular and intertubular dentin.^{6,16–18} These values vary through the thickness of dentin and at different locations in the tooth. Little is known about how these differences in the dentin substrate influence the infiltration of resin monomers. Previous micro-Raman studies on adhesive/dentin interfaces were performed using point-by-point mode across an individual line of the interface. These investigations have not provided information about the distribution of resin infiltration as a function of dentin structure. Two-dimensional micro-Raman mapping/imaging provides an important modality in studying the spatial relationships and distributions of the functional or chemical groups of heterogeneous specimens. The purpose of this investigation was to determine at the molecular level the chemical composition of the adhesive/dentin interface and to quantify dentin demineralization and the infiltration of adhesive monomers into the intertubular region of dentin using micro-Raman mapping/imaging technique.

2 Materials and Methods

2.1 Adhesive/Dentin Specimen Preparation

Six extracted unerupted human third molars stored at 4 °C in 0.9% wt/vol NaCl containing 0.002% sodium azide were used. The teeth were collected after the patients' informed consent was obtained under a protocol approved by the University of Missouri-Kansas City adult health sciences institutional review board. The specimen preparation was detailed in previous publications.^{4,14} Briefly, the occlusal one-third of the crown was sectioned perpendicular to the long axis of the tooth by means of a water-cooled low-speed diamond saw (Buehler Ltd., Lake Bluff, Illinois). A uniform smear layer was created on these fractions by abrading the exposed dentin surface with 600-grit silicon carbide under water. The prepared dentin specimens were selected for treatment with Single Bond (SB) adhesive according to manufacturer's instructions. The dentin was etched with 35% phosphoric acid gel (the etching gel was spread on the dentin surface and left to stand undisturbed for 15 s) and rinsed with water; excess water was removed but the dentin surface remained visibly moist. The adhesive was applied and polymerized for 30 s by exposure to visible light. Six prepared teeth were treated with the adhesive; these specimens were stored for a minimum of 24 h in water at 25 °C before further sectioning. These treated dentin surfaces were sectioned perpendicular and parallel to the bonded surface using a water-cooled low-speed diamond saw. Two parallel cuts, 2 mm deep, were made perpendicular to this surface using the diamond saw. The final cut was about 1.5 mm below the flat surface. The final dimension of the slab was 10 mm long, 2 mm thick, and 1.5 mm wide.

2.2 Micro-Raman Spectroscopy

The micro-Raman spectrometer consisted of an argon ion laser beam (514.5 nm) focused through a ×60 Olympus Plan Neofluor water-immersion objective [numerical aperture (NA) 1.2] to a ~1.5- μ m beam diameter. Raman back-scattered light was collected through the objective and resolved with a monochromator. The spectra were recorded with a software-controlled CCD array. The laser power was approximately

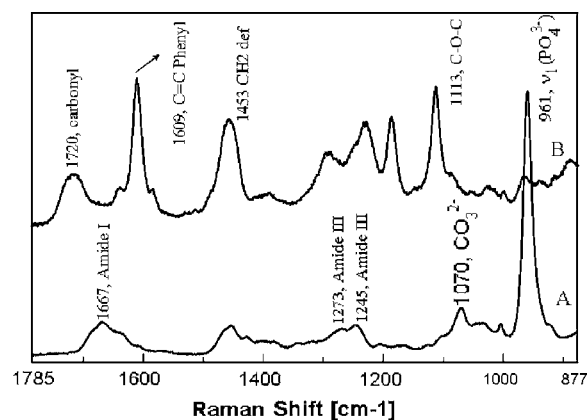


Fig. 1 Raman spectra of dentin (A) and pure SB adhesive resin (B).

3 mW; an imaging system and high-resolution monitor were incorporated to enable visual identification of the position at which the Raman spectrum was obtained. Spectra were Raman-shift-frequency-calibrated using known lines of neon and silicon.

The adhesive/dentin specimen was placed at the focus of a 60× water immersion objective and covered with distilled water in preparation for micro-Raman spectroscopic analysis. Spectra were acquired at positions corresponding to 1- μ m intervals across the adhesive/dentin interface using the computer controlled *x-y-z* stage with a minimum step width of 50 nm. Spectra were obtained at a resolution of ~6 cm^{-1} over the spectral region of 875 to 1785 cm^{-1} and with an integration time of 60 s. Multiple sites across the interface of each specimen were examined spectroscopically. The optical microscope enables visual identification of the position at which the Raman spectrum is obtained. Overlap of the spectra from these sites confirmed the reproducibility of the technique. No postprocessing of the data was performed.

3 Results

3.1 Raman Spectra of Adhesive and Dentin

The Raman spectra of the SB adhesive resin and dentin are shown in Fig. 1. In dentin spectrum, the bands associated with collagen occur at 1667 (amide I), 1273 (amide III), and 1245 cm^{-1} (amide III), the bands associated with mineral occur at 1070 (carbonate) and 961 cm^{-1} (P—O). The SB adhesive is a one-bottle bonding agent consisting of both hydrophilic (HEMA) and hydrophobic (BisGMA) components (Table 1). The intense bands associated with the SB adhesive occur at 1720 (carbonyl), 1609 (phenyl C=C), 1453 (CH_2 def), and 1113 cm^{-1} (C—O—C). These bands are associated with methacrylate monomers in the bonding liquid. In particular, the bands at 1609 and 1113 cm^{-1} are associated with the BisGMA monomer. The Raman intensities at 1453 and 1113 cm^{-1} , which are associated with all monomers in the adhesive and BisGMA monomer in the adhesive, respectively, were used to monitor the adhesive concentration as a function of position across the interface.

Table 1 Description of commercial adhesive SB.

Product and Manufacturer (wt%)	Etchant	Bonding Agent	Concentration
SB (resin/solvent)	35% phosphoric acid gel	HEMA (hydroxyethyl methacrylate)	45/55
3M ESPE (St. Paul, Minnesota)		BisGMA (bisphenol A diglycidyl methacrylate)	
		Polyalkenoic acid	
		Water	
		Ethanol	

3.2 Two-Dimensional Raman Imaging of the Adhesive/Dentin Interface

Figure 2 represents the visible image of the adhesive/dentin interface. There was sufficient contrast among the adhesive, interface, dentin, and tubules to enable easy identification of the position at which the Raman mapping spectra were obtained. The interface between the adhesive and the dentin layer in the intertubular region was visible in the photomicrograph, and the spectroscopic differences at this interfacial zone were investigated.

Figure 3 shows the Raman microscopic images of SB adhesive/dentin interface collected from a $20 \times 12\text{-}\mu\text{m}^2$ area. The relative intensities of the spectral features associated with the mineral (P—O, 961 cm^{-1}) and adhesive resins, i.e., $1453\text{ (CH}_2\text{)}$ or 1113 (C—O—C) are represented by the color differences. Red represents the highest relative intensity, while black represents the lowest. Images of these three spectral parameters (961 , 1113 , and 1453 cm^{-1}) provide information about the spatial distribution of the mineral (apatite), BisGMA monomer, and adhesive components (both BisGMA and HEMA monomers) across the adhesive/dentin interface. Investigation of all of the images indicates that the interface is not a simple, uniform layer, which is not obvious from observation of the visible images (Fig. 2). Such survey maps of the molecular structure provided a reliable and powerful means of

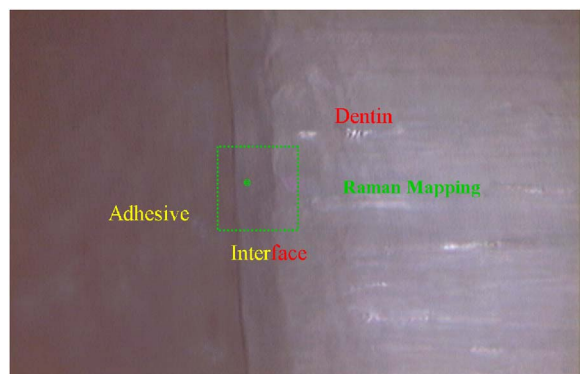


Fig. 2 Visible image of SB adhesive/dentin interface. The spectral mapping was recorded from sites corresponding to the demarcations noted on the image.

identifying dentin demineralization, adhesive monomers distribution, and flaws or defects in the pattern of adhesive penetration. As shown in Fig. 3(a), the image of mineral revealed a partially demineralized layer on the top of dentin substrate. Adhesive monomers readily penetrated into dentin tubules and spread into intertubular region through open tubules [Fig. 3(b)]. The diffusion of resin monomers (BisGMA and HEMA) differed substantially. In a comparison with HEMA, BisGMA monomer resisted diffusion into the demineralized dentin, especially, the intertubular area [Fig. 3(c)].

3.3 Quantifying Adhesive Diffusion in the Intertubular Region of Dentin

Since the preceding images contained hundreds of very high quality spectra at a resolution of $\sim 1.5\text{ }\mu\text{m}$, the relative composition and other chemical information can be determined across the length and breadth of the adhesive/dentin interface. As an example, a series of micro-Raman mapping spectra across the interface [the position was represented by the dotted line in Fig. 3(c)] are represented in Fig. 4(a). The first five spectra were acquired from pure adhesive, a methacrylate-based polymer. Bands associated with the adhesive and collagen components of dentin were noted in the sixth spectrum. The strong band of P—O group (961 cm^{-1}) in the tenth spectrum suggested the bottom of the demineralized dentin layer. The spectra recorded at the 1- and $4\text{-}\mu\text{m}$ positions in the interface are presented in detail, and major spectral changes are marked with arrows [Fig. 4(b)]. The intensity of the Raman bands attributed to the adhesive (1113 , 1609 , 1720 cm^{-1}) decreased as a function of depth, indicating the gradual decrease of adhesive infiltration into demineralized dentin.

To determine quantitatively the differences in adhesive infiltration into demineralized dentin at different depths, the ratios of the relative integrated intensities of bands associated with adhesive and collagen were calculated. The CH_2 in HEMA and BisGMA (1453 cm^{-1}) and C—O—C in BisGMA monomer (1113 cm^{-1}) were used to monitor the adhesive monomers concentration and the amide I band (1667 cm^{-1}) was selected for collagen. However, the amide I band overlaps the carbonyl and C=C region of the adhesive (Fig. 5). Due to the interaction with the neighboring bands, the following method was used for band area measurement. Difference spectra were calculated by subtracting the spectra of the col-

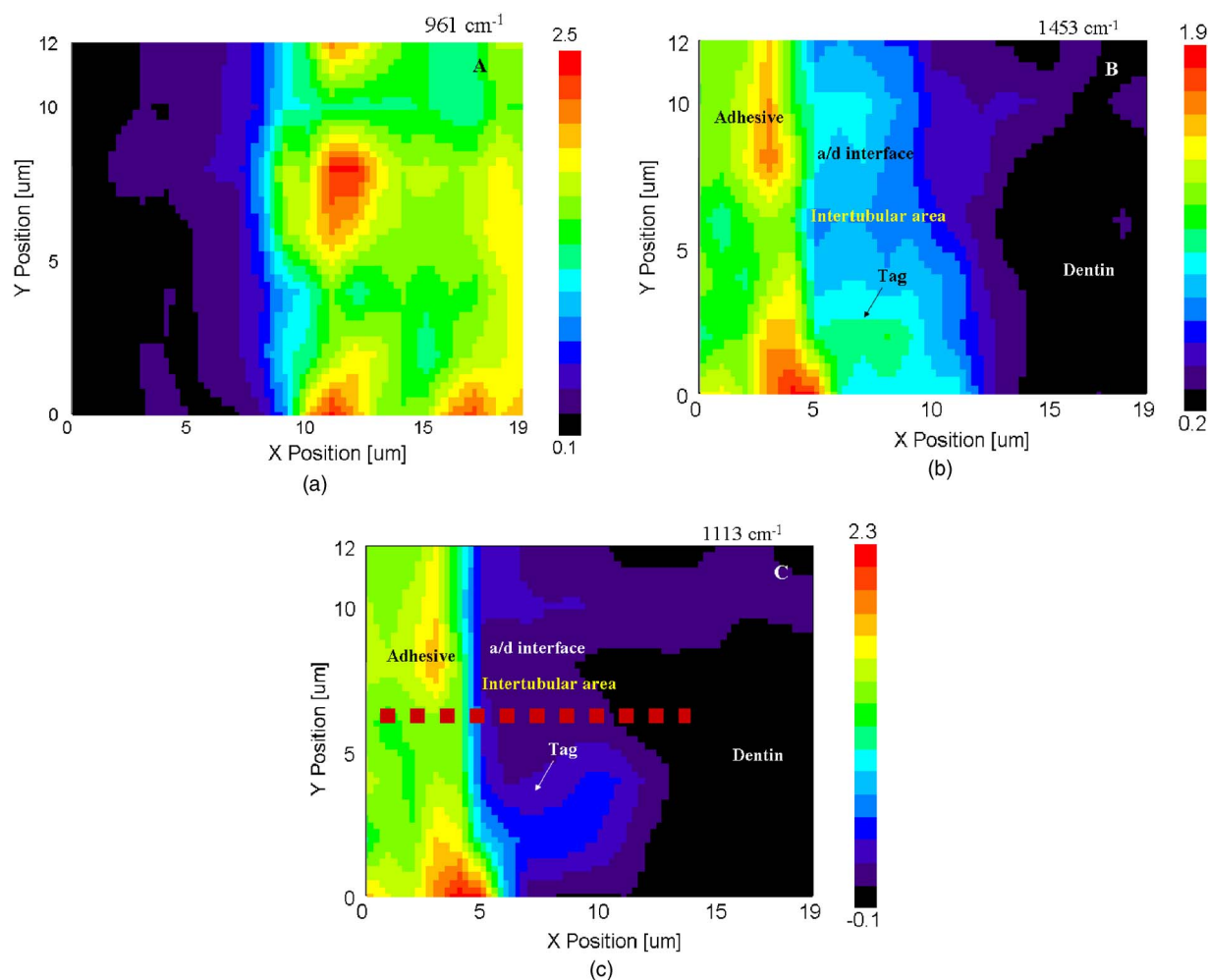


Fig. 3 Micro-Raman spectroscopic images of the SB adhesive/dentin (a/d) interface: (a) 961-cm^{-1} image (phosphate), (b) 1453-cm^{-1} image (CH_2), and (c) 1113-cm^{-1} image (C—O—C).

lagen from the spectra of the interface. For example, the amide I band of the collagen digitally was subtracted from the band presented in the Raman spectra of the interface (Fig. 5). After the band at 1667 cm^{-1} was eliminated, the integrated band areas of the amide I and CH_2 (1453 cm^{-1}) or C—O—C (1113 cm^{-1}) were determined at different positions. Similarly, to determine the extent of dentin demineralization, the ratios of the relative integrated intensities of the spectral features from the mineral (961 cm^{-1} , P—O) and collagen (1454 cm^{-1}) (mineral/matrix ratios) were calculated. The depth of the demineralized and/or the partially demineralized layer was determined.

Figure 6 represents the adhesive monomers penetration and degree of dentin demineralization as a function of depth in the intertubular region of dentin. The adhesive monomer penetration and degree of demineralization across the interface were combined in one figure. The interfacial profile of adhesive monomer penetration and depth of demineralization were clearly observed. As shown in Fig. 6, dentin was not completely demineralized across the interface, which was mainly demineralized to a depth of ~ 3 to $4\ \mu\text{m}$ and the depth of partially demineralized dentin was $\sim 3\ \mu\text{m}$. The ratios of $1453/1667$ for adhesive monomers/collagen as a func-

tion of spatial position showed a gradual decline, while the ratios of $1113/1667$ (BisGMA/collagen) showed a dramatic decrease in the concentration of BisGMA monomer across the adhesive/dentin interface.

4 Discussion

The micro-Raman mapping/imaging technique is a powerful means for obtaining chemical images of the adhesive/dentin interface. By combining Raman spectroscopy with microscopy, a comprehensive representation of the degree and depth of demineralization, distribution of adhesive resin monomers, and width of the interface can be obtained with great spatial resolution at the microscopic level. A distinct advantage is that specimens can be analyzed directly, in air, at room temperature and pressure, wet or dry without destroying the specimen.

In this paper, the spectral data was recorded from samples that were wet throughout the analysis. Collecting spectral data from the demineralized dentin under wet conditions reduces the potential for collagen collapse as a result of drying/desiccation, since such collapse would lead to inaccurate characterization of the extent or degree of dentin demineralization.

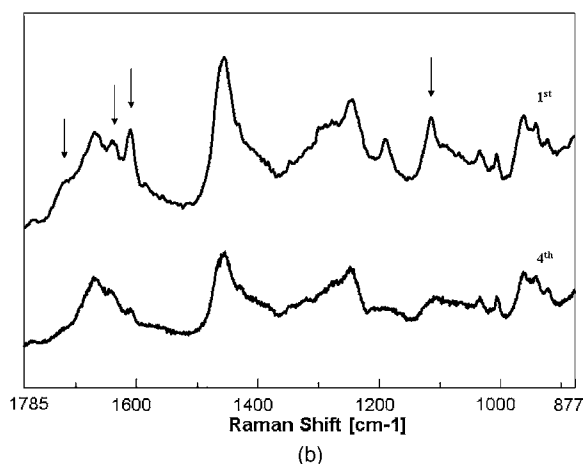
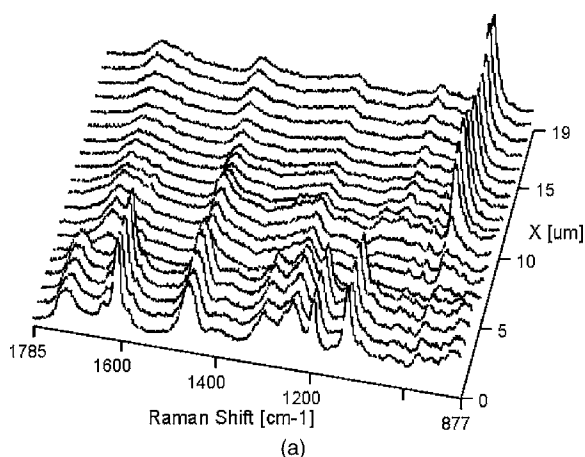


Fig. 4 (a) Raman mapping spectra acquired at 1- μm intervals across intertubular area of SB adhesive/dentin interface and (b) the spectra recorded at the 1- and 4- μm depths in the adhesive/dentin interface. Major spectral changes are marked with arrows.

Water immersion also reduces the potential that the sample will be exposed to excess and potentially damaging heat during spectral imaging. On the other hand, unlike IR spectroscopy, water does not present a strong Raman signal within the biological fingerprint region, thus, compound specific molecules can be identified in hydrated dentin samples without processing the data to remove spectral interferences from water.^{19,20} The results of our Raman study provided the direct evidence of the variable composition and structure of the resin-collagen biopolymer hybrid layer across the breadth of the adhesive/dentin interface. This 3 to 5- μm hybrid layer is not a uniform, structurally integrated biopolymer layer, but instead a layer with a gradient, complex structure, which is dramatically influenced by permeability of substrates and diffusion of monomers.

The permeability of dentin substrates to monomers and the monomer diffusivity into the substrates are essential factors for the bonding of resins to dentin. A mineralized dentinal matrix is relatively impermeable to resin monomers. Acid etching of dentin removes the mineral phase and increases the porosities of the substrates. Resin monomers can enter demineralized dentin via tubules and via spaces around the collagen fibrils of intertubular dentin surfaces (Fig. 7). The

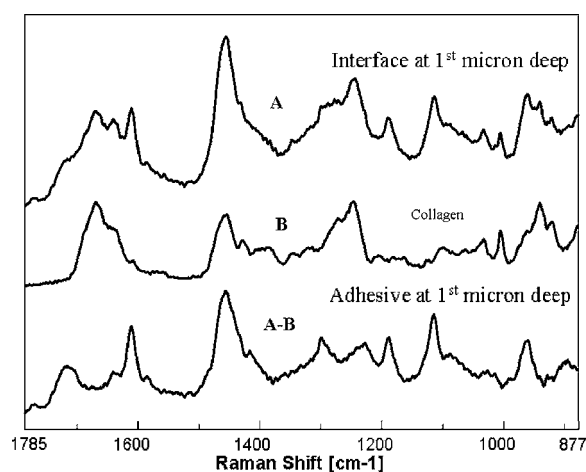


Fig. 5 Micro-Raman spectrum from the 1- μm depth in the adhesive/dentin interface. Separation of collagen and adhesive spectra for relative content calculation through spectral subtraction.

diffusion and/or distribution of adhesive monomers into the interface have been directly observed using micro-Raman imaging (Fig. 3). Adhesive monomers readily penetrated into dentinal tubules, which also served as avenues for infiltration of suitable monomers into the intertubular regions. However, there was a distinct difference in the resin monomer penetration between the regions close to tubules and the regions away from tubules in the intertubular dentin. For example, the extent of adhesive (BisGMA/HEMA) monomer penetration was higher in the intertubular regions close to tubules as compared to the middle regions between the tubules.

The discrepancy between the depth of demineralization and that of resin monomer penetration in the intertubular regions of the adhesive/dentin interfaces were clearly observed by combining the adhesive monomer infiltration and degree of demineralization as a function of position across the interface into one figure (Fig. 6). This method provided a quantitative representation of the degree of resin monomer penetration and a comprehensive chemical pattern across the adhesive/dentin

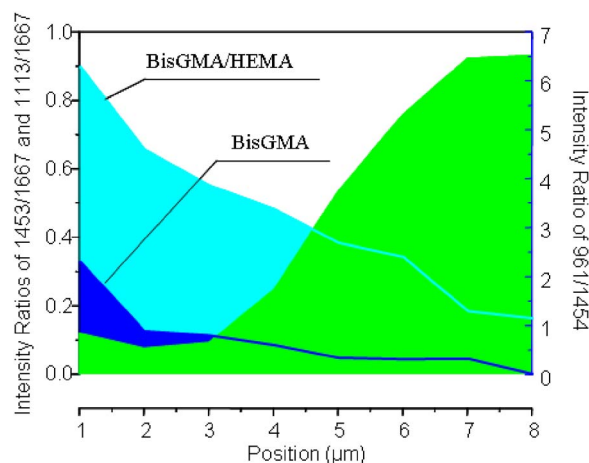


Fig. 6 Raman intensity ratios of 1453/1667, 1113/1667, and 961/1454 as a function of spatial position across the adhesive/dentin interface.

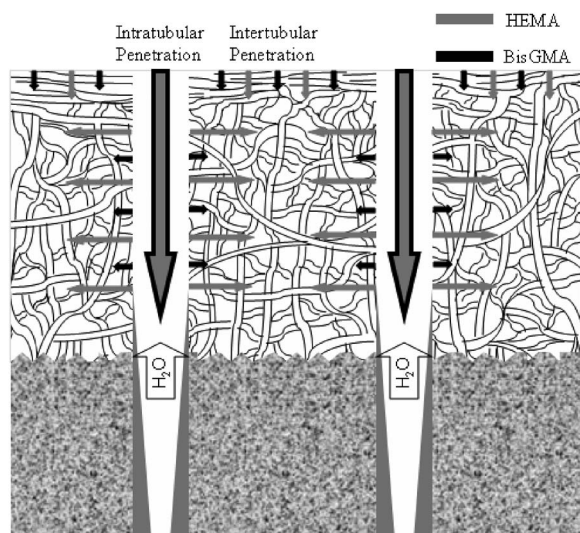


Fig. 7 Schematic representation of adhesive monomers infiltrating into demineralized dentin substrate via intertubular diffusion from the dentin surface and/or intratubular diffusion in tubules.

interface. There was a marked difference in the degree of penetration of HEMA and BisGMA monomers. In comparison to the hydrophilic HEMA monomer, the BisGMA monomer resisted diffusion into the demineralized intertubular dentin area.

The differences in resin monomer diffusion are likely due to the adhesive phase separation as it interacts with the wet demineralized dentin matrix.^{21,22} With wet bonding techniques, the dentin tubules and spaces between the demineralized collagen fibrils are filled with water. It is through these water-filled spaces and tubules that adhesive monomer must penetrate if it is to infiltrate the demineralized dentin matrix. As reported in a recent study, the adhesive may separate into hydrophobic BisGMA-rich and hydrophilic HEMA-rich phases as it interacts with water.²¹ Hydrophobic monomers, such as BisGMA in SB adhesive, would resist diffusing into the sites where there is residual water. Phase separation of the adhesive that infiltrates the demineralized dentin matrix would compromise the structural integrity of the resultant hybrid layer. In contrast to an impervious 3-D polymer/collagen network, adhesive phase separation would lead to a very porous hybrid layer characterized by a minimal amount of the hydrophobic BisGMA distributed in a hydrophilic HEMA-rich matrix. Because of its low cross-link density, HEMA is unstable in aqueous environments, and thus, this phase will degrade when exposed to oral fluids.²³ This may explain the decreased bond strength of the adhesive/dentin interface in aqueous environments over the long term. The results indicated that although the “wet” bonding technique provided spaces for adhesive monomer to diffuse, several other factors interfered with adhesive penetration into the demineralized dentin layer.

Raman microspectroscopy is an exceptional tool for investigating the chemistry of the heterogeneous interfaces because it does not rely on homogenization, extraction, or dilution but rather each structure is analyzed *in situ*. As shown in the spectral results, we did not experience spectral interference

from fluorescence. The lack of any interference from fluorescence may be attributable in part to the improved confocal signal detection and short integration time. Because we do not experience the background fluorescence that previous authors have described, we can present our data without any postprocessing. This is a critical attribute and feature of our studies since many of the rules for postprocessing spectral data are open to interpretation by the independent investigator and thus, such data processing can introduce features that are not necessarily representative of the sample under investigation.

In summary, micro-Raman imaging was shown to be a remarkable tool for studying heterogeneous interfaces like adhesive/dentin specimens. This paper provided clear spectroscopic evidence of distinct differences in the degree of adhesive penetration and distribution of each monomer in the intertubular regions between tubules. The interaction of tissues and biomaterials at biologic interfaces is extremely important. The micro-Raman imaging technique could be used for comprehensive characterization of these chemical/physical reactions that occur at the tissue/biomaterial interfaces.

Acknowledgments

This investigation was supported by U.S. Public Health Service (USPHS) Research Grants DE 015281 (YW), DE 15735 (YW), and DE014392 (PS) from the National Institute of Dental and Craniofacial Research, National Institutes of Health, Bethesda, Maryland. The authors gratefully acknowledge 3M ESPE, Dental Products Division, for donating the dentin adhesive products used in this study.

References

1. J. D. Eick, A. J. Gwinnett, D. H. Pashley, and S. J. Robinson, “Current concepts on adhesion to dentin,” *Crit. Rev. Oral Biol. Med.* **8**, 306–335 (1997).
2. N. Nakabayashi, K. Kojima, and E. Masuhara, “The promotion of adhesion by the infiltration of monomers into tooth substrates,” *J. Biomed. Mater. Res.* **16**, 265–273 (1982).
3. N. Nakabayashi and Y. Saimi, “Bonding to intact dentin,” *J. Dent. Res.* **75**, 1706–1715 (1996).
4. P. Spencer, Y. Wang, M. P. Walker, D. M. Wieliczka, and J. R. Swafford, “Interfacial chemistry of the dentin/adhesive bond,” *J. Dent. Res.* **79**, 1458–1463 (2000).
5. Y. Wang and P. Spencer, “Hybridization efficiency of the adhesive dentin interface with wet bonding,” *J. Dent. Res.* **82**, 141–145 (2003).
6. D. H. Pashley, B. Ciucchi, H. Sano, and J. A. Horner, “Permeability of dentin to adhesive agents,” *Quintessence Int.* **24**, 618–631 (1993).
7. A. J. Gwinnett, “Quantitative contribution of resin infiltration/hybridization to dentin bonding,” *Am. J. Dent.* **6**, 7–9 (1993).
8. J. Kanca, “Improved bond strength through acid etching of dentin and bonding to wet dentin surfaces,” *J. Am. Dent. Assoc.* **123**, 235–243 (1992).
9. A. J. Gwinnett, “Dentin bond strength after air drying and rewetting,” *Am. J. Dent.* **7**, 144–148 (1994).
10. L. E. Tam and R. M. Pilliar, “Fracture surface characterization of dentin-bonded interfacial fracture toughness specimens,” *J. Dent. Res.* **73**, 607–619 (1994).
11. M. F. Burrow, M. Satoh, and J. Tagami, “Dentin durability after three years using a dentin bonding agent with and without priming,” *Dent. Mater.* **12**, 302–307 (1996).
12. M. Hashimoto, H. Ohno, M. Kaga, K. Endo, H. Sano, and H. Oguchi, “*In vivo* degradation of resin-dentin bonds in humans over 1 to 3 years,” *J. Dent. Res.* **79**, 1385–1391 (2000).
13. P. Spencer, Y. Wang, M. P. Walker, and J. R. Swafford, “Molecular structure of acid-etched dentin smear layers—*in situ* study,” *J. Dent. Res.* **80**, 1802–1807 (2001).
14. Y. Wang and P. Spencer, “Quantifying adhesive penetration in adhesive/dentin interface using confocal Raman microspectroscopy,”

- J. Biomed. Mater. Res.* **59**, 46–55 (2002).
15. Y. Wang and P. Spencer, "Analysis of acid-treated dentin smear debris and smear layers using confocal Raman microspectroscopy," *J. Biomed. Mater. Res.* **60**, 300–308 (2002).
 16. M. Yoshiyama, R. Carvalho, H. Sano, J. Horner, P. D. Brewer, and D. H. Pashley, "Interfacial morphology and strength of bonds made to superficial *versus* deep dentin," *Am. J. Dent.* **8**, 297–302 (1995).
 17. M. Yoshiyama, R. M. Carvalho, H. Sano, J. A. Horner, P. D. Brewer, and D. H. Pashley, "Regional bond strengths of resins to human root dentine," *J. Dent.* **24**, 435–442 (1996).
 18. T. Yoshikawa, H. Sano, M. F. Burrow, J. Tagami, and D. H. Pashley, "Effects of dentin depth and cavity configuration on bond strength," *J. Dent. Res.* **78**, 898–905 (1999).
 19. P. Spencer, Y. Wang, J. L. Katz, and A. Misra, "Physicochemical interactions at the dentin/adhesive interface using FTIR chemical imaging," *J. Biomed. Opt.* **10**, 031104 (2005).
 20. G. Eliades, G. Vougiouklakis, and G. Palaghias, "Effect of dentin primers on the morphology, molecular composition and collagen conformation of acid demineralized dentin *in situ*," *Dent. Mater.* **15**, 310–317 (1999).
 21. P. Spencer and Y. Wang, "Adhesive phase separation at the dentin interface under wet bonding conditions," *J. Biomed. Mater. Res.* **62**, 447–456 (2002).
 22. Y. Wang and P. Spencer, "Overestimating hybrid layer quality in polished adhesive/dentin interfaces," *J. Biomed. Mater. Res.* **68A**, 735–746 (2004).
 23. D. M. Yourtee, R. E. Smith, K. A. Russo, S. Burmaster, J. M. Cannon, J. D. Eick, and E. L. Kostoryz, "The stability of methacrylate biomaterials when enzyme challenged: kinetic and systematic evaluations," *J. Biomed. Mater. Res.* **57**, 523–531 (2001).